Galactic Evolution

Galactic Evolution

Evidence of galaxy interactions in clusters of galaxies

- In rich, regularly shaped clusters we find a large fraction of elliptical galaxies.
- Since regularly shaped clusters are thought to be old there has been enough time for mergers.
- Typically, the merger of spirals will lead to an elliptical.
- The fraction of spirals is also larger near the center of clusters where the probability of collisions is larger.

FIGURE 26.1 The center of the Coma cluster. The width of this view is about 18 arcmin. (Courtesy of National Optical Astronomy Observatories.)

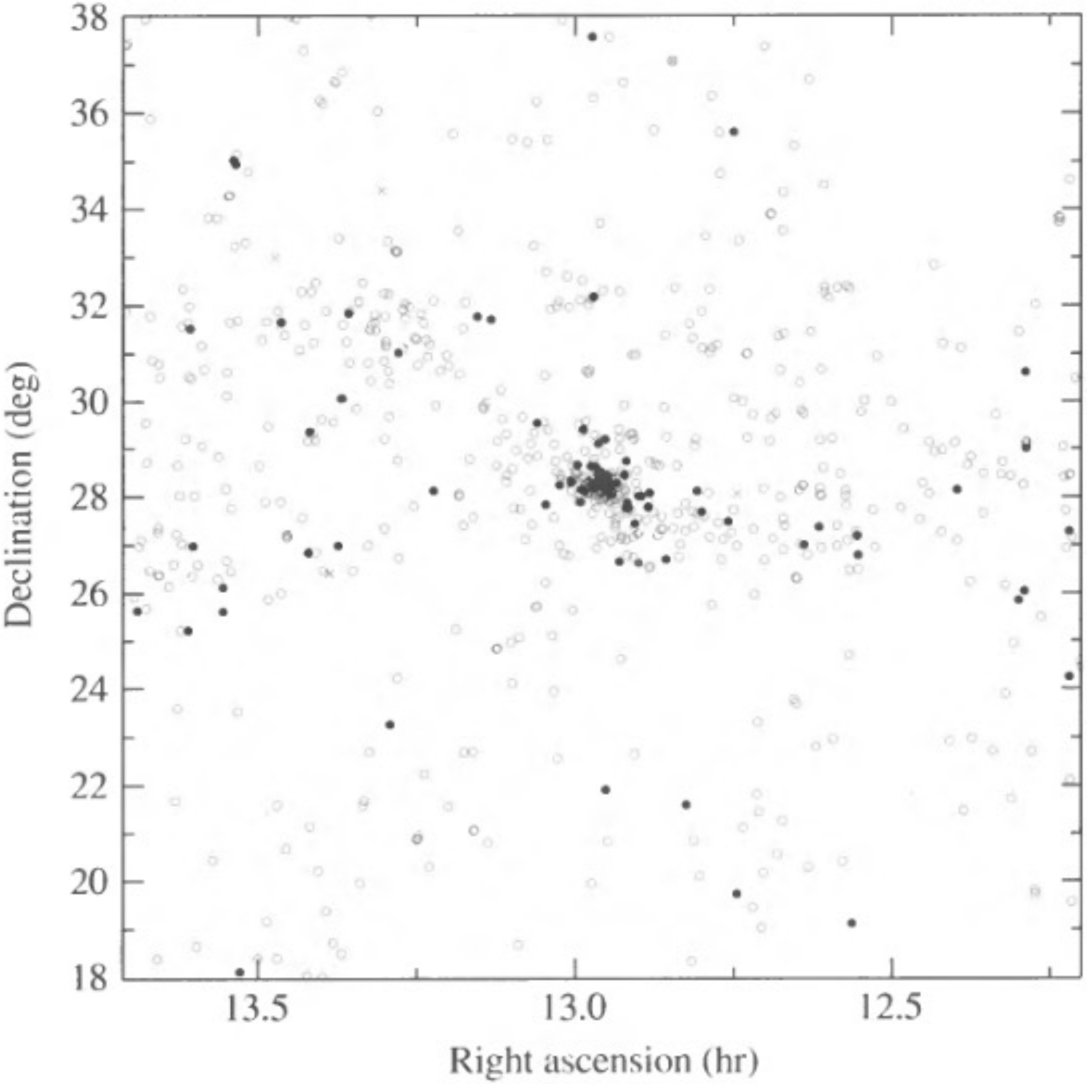

FIGURE 26.2 The Coma cluster of galaxies, showing the ellipticals (filled circles) and spirals (open circles). Note that the scale is much larger than the width of the image in Fig. 26.1.

FIGURE 26.3 The Hercules cluster of galaxies. (Courtesy of National Optical Astronomy Observatories.)

Galactic Evolution

Evidence of galaxy interactions: Warped Disks, Stripping of gas, and increased star formation

- Warped disk are observed in a large fraction of disk galaxies.

- The warped disked are thought to be due to tidal interactions with smaller satellite galaxies.

- Stripping of gas during galaxy interactions

- Interactions may trigger star formation. This in turn will increase the supernova rate, leading to galactic superwinds, capable of liberating a large amount of gas from the galaxy.

Our Milky Way isn’t the only warped galaxy. This galaxy – labeled ESO 510-G13 – is an edge-on warped spiral galaxy. Similar to the Milky Way it has a pronounced warp in its gaseous disk and a less pronounced warp in its disk of stars.

The spiral galaxy, NGC4402, is currently falling towards the centre of the Virgo cluster (downwards in this image). The bowed and truncated disk, and the concentration of dust and gas to one side of the galaxy are all indicators that ram pressure stripping is forcing gas out of the galaxy.

M82 starburst galaxy taken by the Hubble Telescope, combining exposures taken with four colored filters that capture starlight from visible and infrared wavelengths as well as the light from the glowing hydrogen filaments.

FIGURE 26.4 The plumes on the opposite sides of NGC 520 are evidence of a tidal interaction, possibly ending in the merger of the two colliding disk galaxies. Note the diagonally oriented dust lane. (Courtesy of Gemini Observatory/AURA.)

Dynamical Friction

When galaxies collide collisions between stars are very rare because stars are so far apart. **Interaction between stars are gravitational in nature.**

Imagine a globular cluster or small galaxy of **mass M** and **velocity $\mathbf{v_M}$** moving through stars, gas, dust and dark matter with as density of $\rho(r)$.

The gravitational interaction between the globular cluster and the background mass results in a force opposing the motion of the globular cluster. This force is referred to as **Dynamical Friction**.

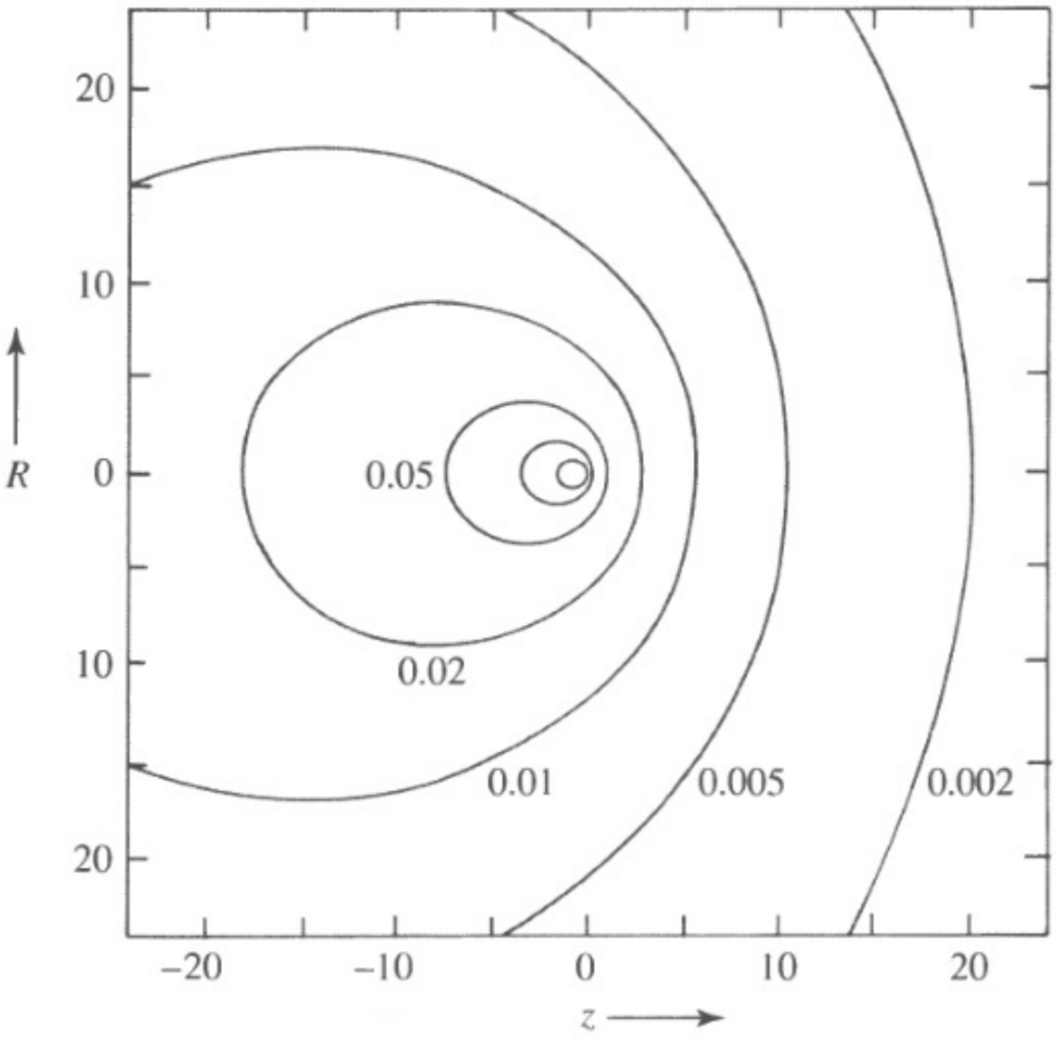

FIGURE 26.5 The fractional enhancement in the density of stars caused by the motion of a mass M in the positive z direction. (Figure adapted from Mulder, *Astron. Astrophys.*, *117*, 9, 1983.)

Dynamical friction

$f_d \cong \frac{cG^2M^2\rho}{v_M^2}$ (1),

M, v_m are the mass and velocity of the GC. ρ is the density of the background mass

GCs will fall to the center of the galaxy because of dynamical friction

For a flat rotation curve we have: $\rho(r) \cong \frac{v_M^2}{4\pi G r^2}$ (2)

$$(1) \wedge (2) \Longrightarrow f_d \cong \frac{cG^2M^2}{v_M^2}\frac{v_M^2}{4\pi G r^2} = \frac{cGM^2}{4\pi r^2}$$

The angular momentum of the globular cluster about the z direction is $L_z = Mv_M r$

The torque on the GC from the frictional force is $\vec{\tau} = \vec{r}\times\overrightarrow{F_d} \Longrightarrow \tau_z = rf_d$

$$\tau = \frac{dL}{dt} \Longrightarrow rf_d = Mv_M\frac{dr}{dt} \Longrightarrow r\frac{cGM^2}{4\pi r^2} = Mv_M\frac{dr}{dt} \Longrightarrow t_C = \frac{2\pi v_M r_i^2}{cGM}$$

where t_c is the age of the globular cluster.

Dynamical friction

Within the cluster lifetime t_c all globular clusters within a radius of $r < r_i$ will have spiraled to the center.

$$r_{max} = r_i = \sqrt{\frac{cGMt_C}{2\pi v_M}}$$

where t_c is the age of the globular cluster and M is its mass.

Example: Consider a globular cluster in M31. Assume $M_{GC} = 5 \times 10^6$ $M_\odot$ and $v_M = 250$km/s. If t_c=13 Gyr then r_{max}~3.7 kpc. Any globular cluster within 3.7 kpc will have spiraled into the nucleus by now!

Note that r_{max} scales as $M^{1/2}$ so the “cleared out” radius is larger for more massive globular clusters.

Rapid Galaxy Encounters

If the collision of two galaxies is so rapid that their stars don't have time to respond, there is almost no dynamical friction.

In a rapid collision the **potential energy** of the galaxies after the collision is **unchanged** but the **internal kinetic energies** of the galaxies has **increased.** *Before the collision and after relaxation the virial theorem applies*.

Before Collision: internal kinetic, potential and total energies K_i, U_i, E_i
$-2K_i = U_i$ and $E_i = K_i + U_i \Rightarrow -2K_i = E_i - K_i \Rightarrow K_i = -E_i$

Just After Collision Galaxy is out of Equilibrium:
$K_i \Rightarrow K_i + \Delta K$, $U_i \Rightarrow U_i$ and $E_f = E_i + \Delta K$

After some relaxation time the Galaxy is back in Equilibrium:
$-2K_f = U_f$ and $E_f = K_f + U_f \Rightarrow K_f = -E_f = -E_i - \Delta K \Rightarrow K_f = K_i - \Delta K$

$U_f = -2K_f = -2K_i + 2\Delta K = U_i + 2\Delta K \Rightarrow U_f = U_i + 2\Delta K$

Rapid Galaxy Encounters

Question: So how does the galaxy redistribute K and U during relaxation so that K decreases by 2ΔK just after the collision?

Answer: the potential energy increases by the same amount. This can happen by the galaxy expanding and/or producing rings.

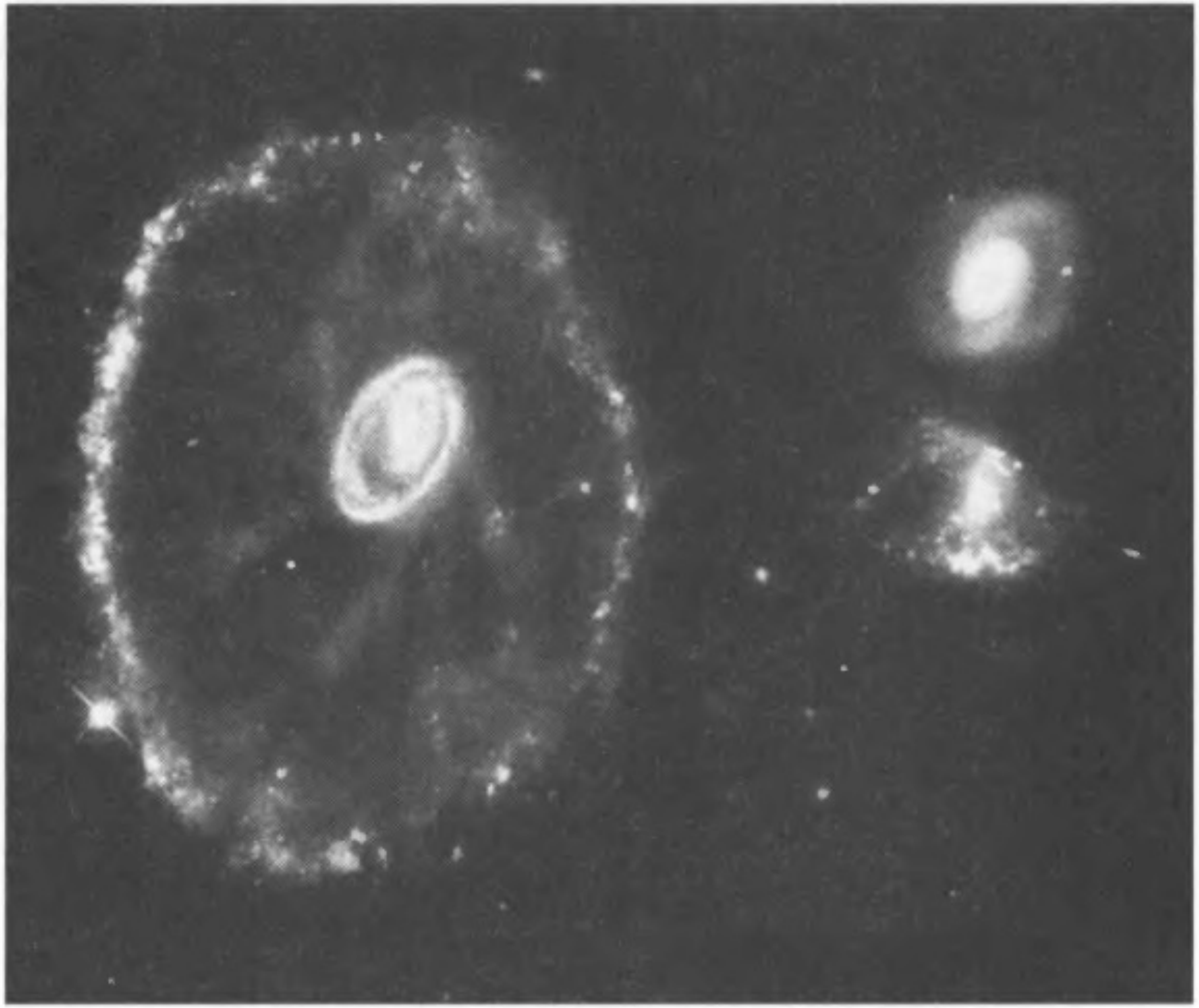

FIGURE 26.6 An HST image of the ring galaxy known as the Cartwheel (A0035−335). The diameter of the ring is about 46 kpc. As the ring expands at 89 km s^{-1}, it triggers bursts of star formation. It is not clear which of the two galaxies at right may have been the intruder. [Courtesy of Kirk Borne (STScI), and NASA.]

FIGURE 26.7 The polar-ring galaxy NGC 4650A. [Courtesy of J. Gallagher (University of Wisconsin–Madison) and the Hubble Heritage Team (AURA/STScI/NASA).]

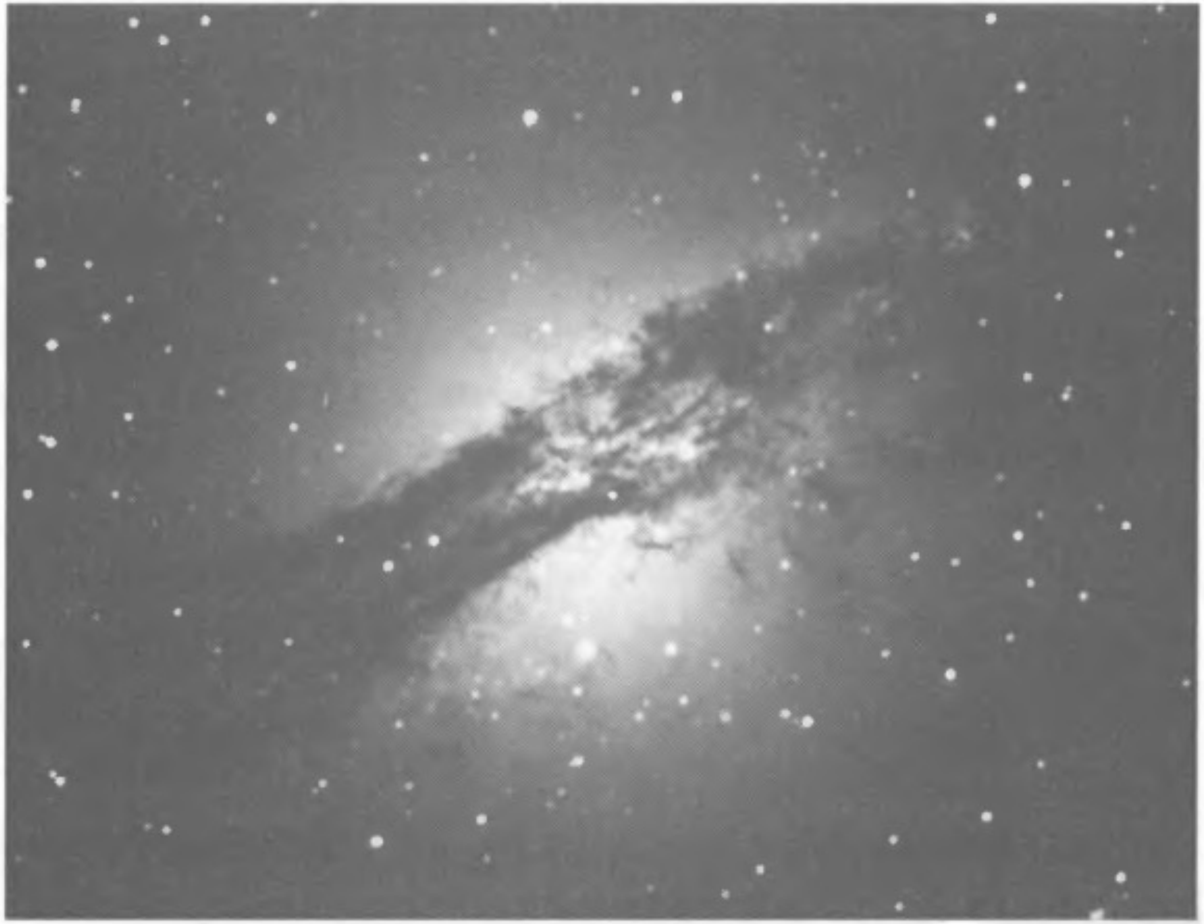

FIGURE 26.8 Centaurus A (NGC 5128) is a dust-lane elliptical galaxy. (Courtesy of NOAO Cerro Tololo Interamerican Observatory.)

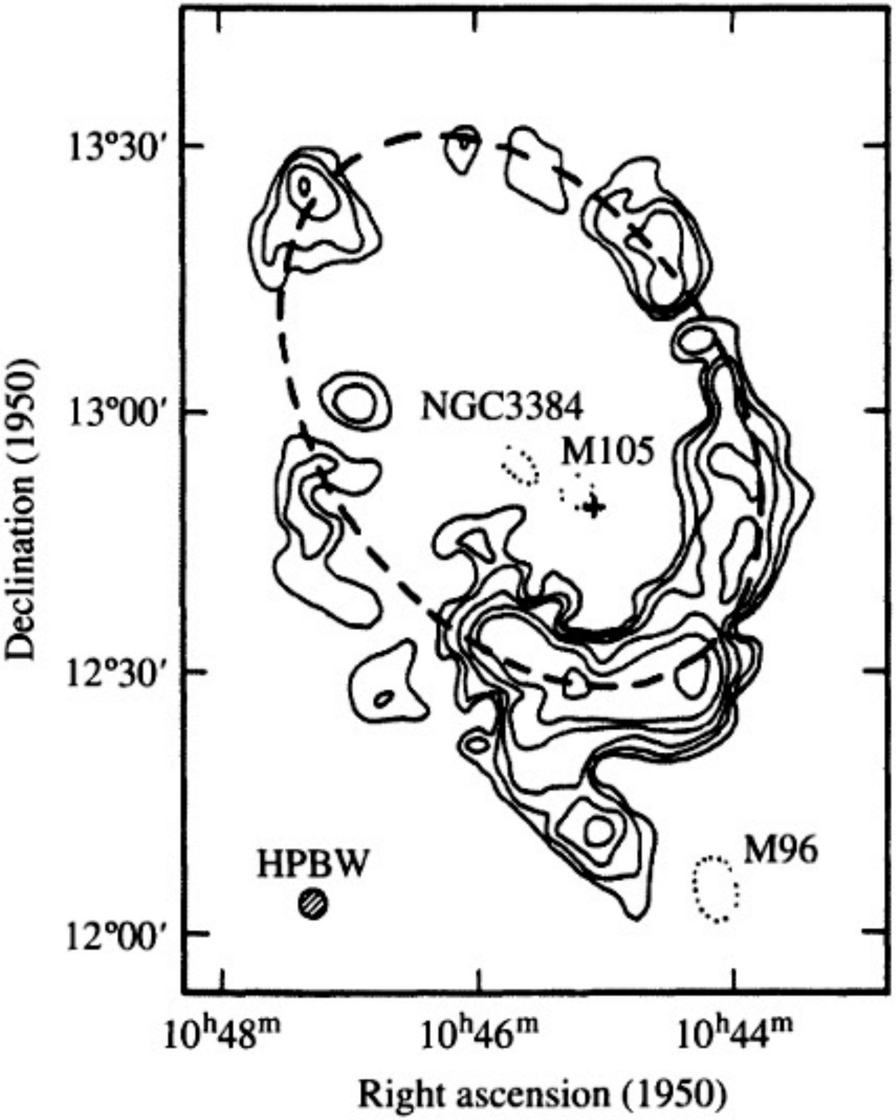

FIGURE 26.9 21-cm radio contours showing the ring of neutral hydrogen around the galaxies M105 (a giant elliptical) and NGC 3384 (an S0) in the M96 group. Note that the ring is more than 1° wide on the sky. (Figure adapted from Schneider, *Warped Disks and Inclined Rings around Galaxies*, Cambridge University Press, Cambridge, 1991.)

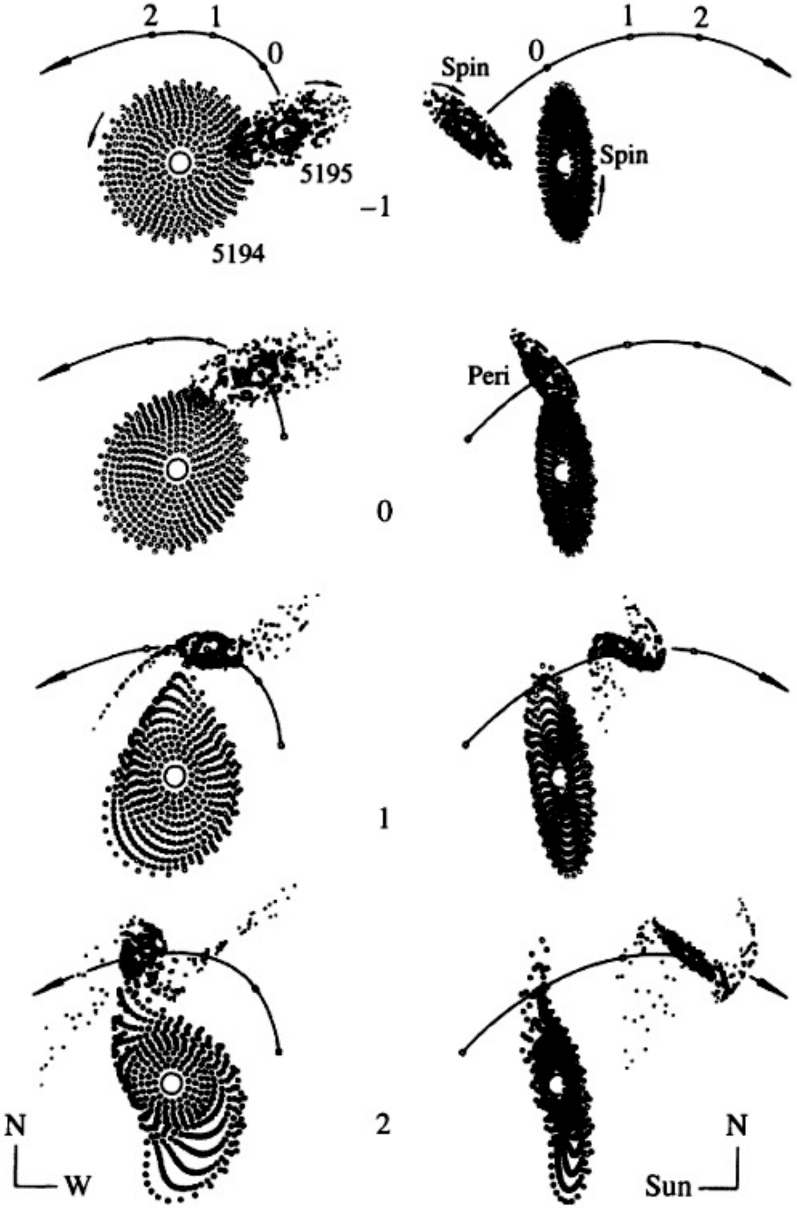

FIGURE 26.10 The Toomres' computer simulation of the interaction between M51 (NGC 5194) and NGC 5195. Note from the side view that the "bridge" does not actually connect the two galaxies. You may also note the resulting warped disk. [Figure adapted from Toomre, *The Large Scale Structure of the Universe*, Longair and Einasto (eds.), Reidel, Dordrecht, 1978.]

FIGURE 26.11 The Antennae galaxies, NGC 4038 and NGC 4039, and their tidal tails. [Courtesy of Brad Whitmore (STScI) and NASA.]

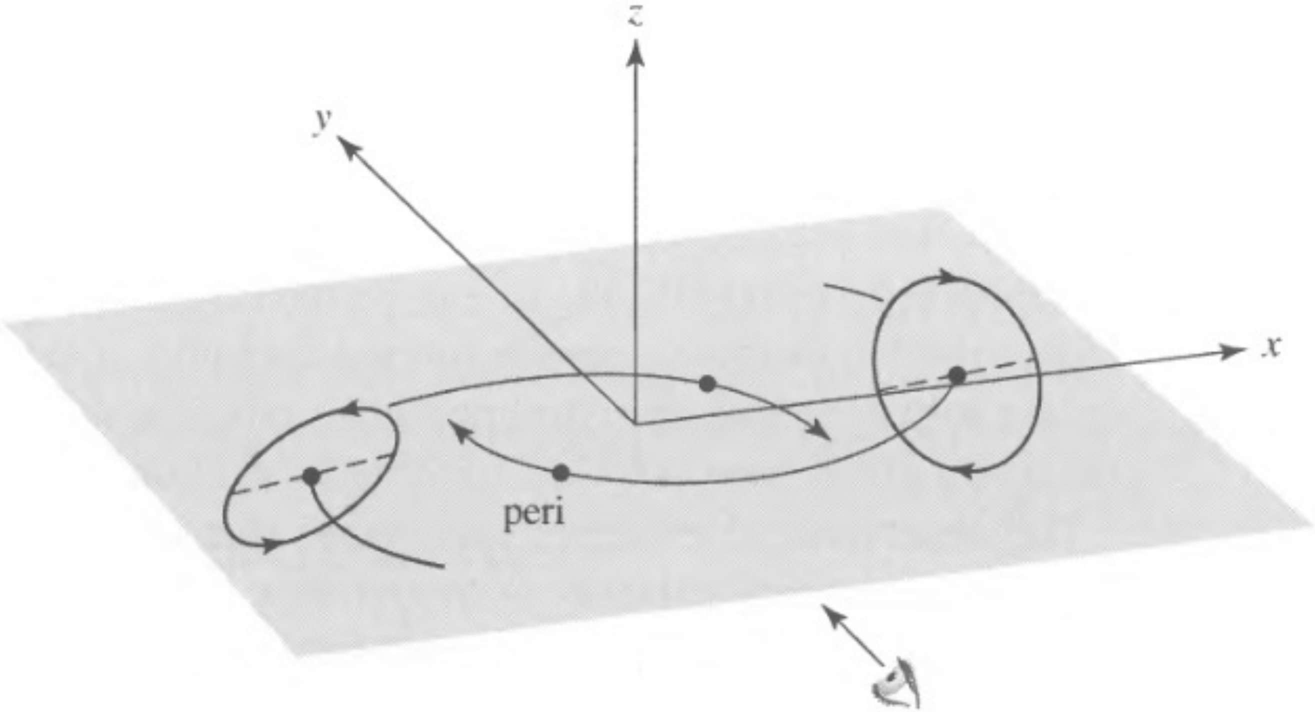

FIGURE 26.12 The orbital geometry used to calculate the formation of the tidal-tail galaxies shown in Fig. 26.11. The disks are shown in their initial positions. Each disk is initially inclined by 60° to the orbital plane, and a dashed line indicates the intersection of each disk with the orbital plane. The positions of closest approach are identified ("peri"). The viewing direction for Fig. 26.13 is indicated as along the positive y-axis. (Figure adapted from Barnes, *Ap. J.*, *331*, 699, 1988.)

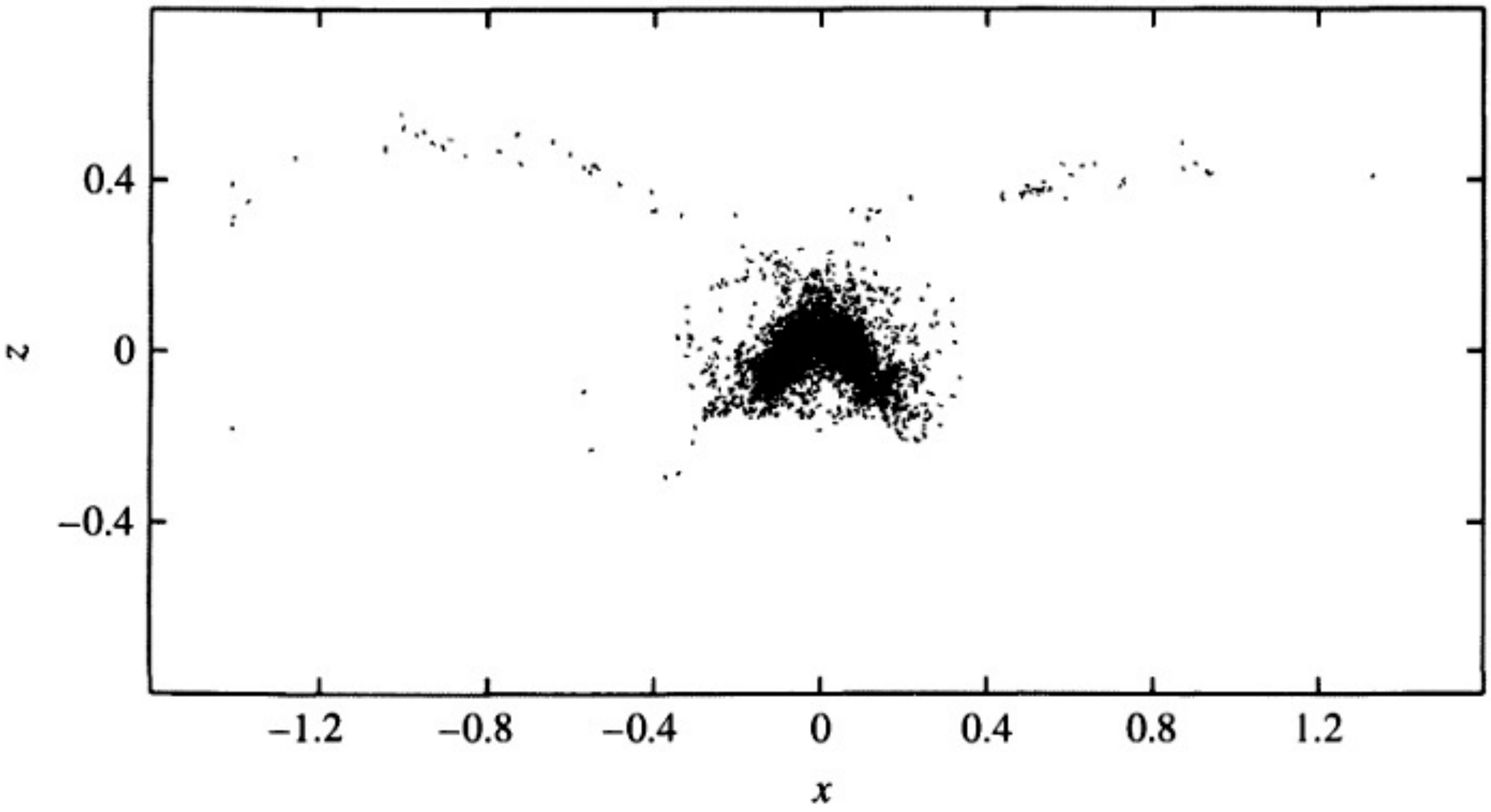
0.4
0
−0.4
z
−1.2
−0.8
−0.4
0
0.4
0.8
1.2
x

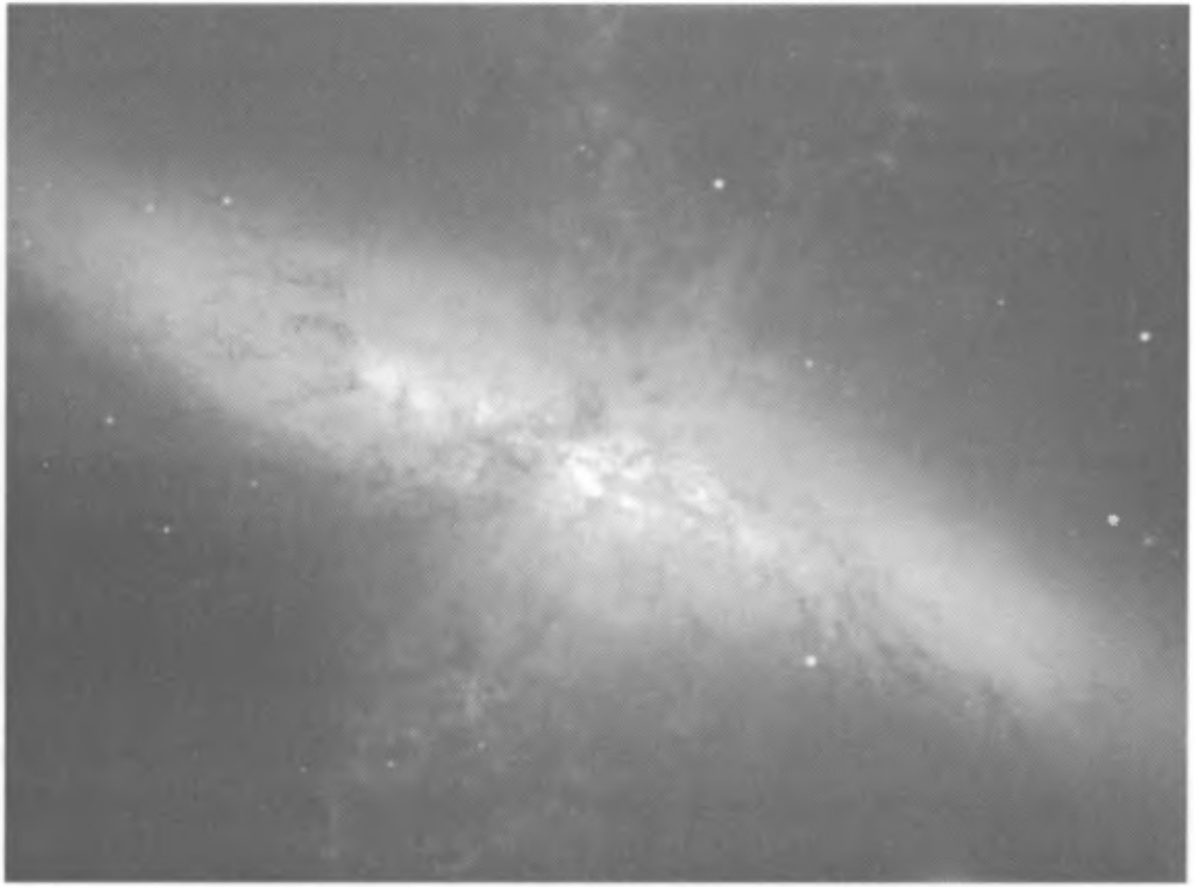

FIGURE 26.14 The starburst galaxy M82 (NGC 3034). This composite image was obtained by the Subaru Telescope's FOCAS instrument in B, V, and Hα wavelengths. [Courtesy of National Astronomical Observatory of Japan (NAOJ).]

FIGURE 26.15 The passage of three small galaxies through a giant elliptical in the cluster Abell 2199. (Courtesy of Whipple Observatory and Harvard CfA.)

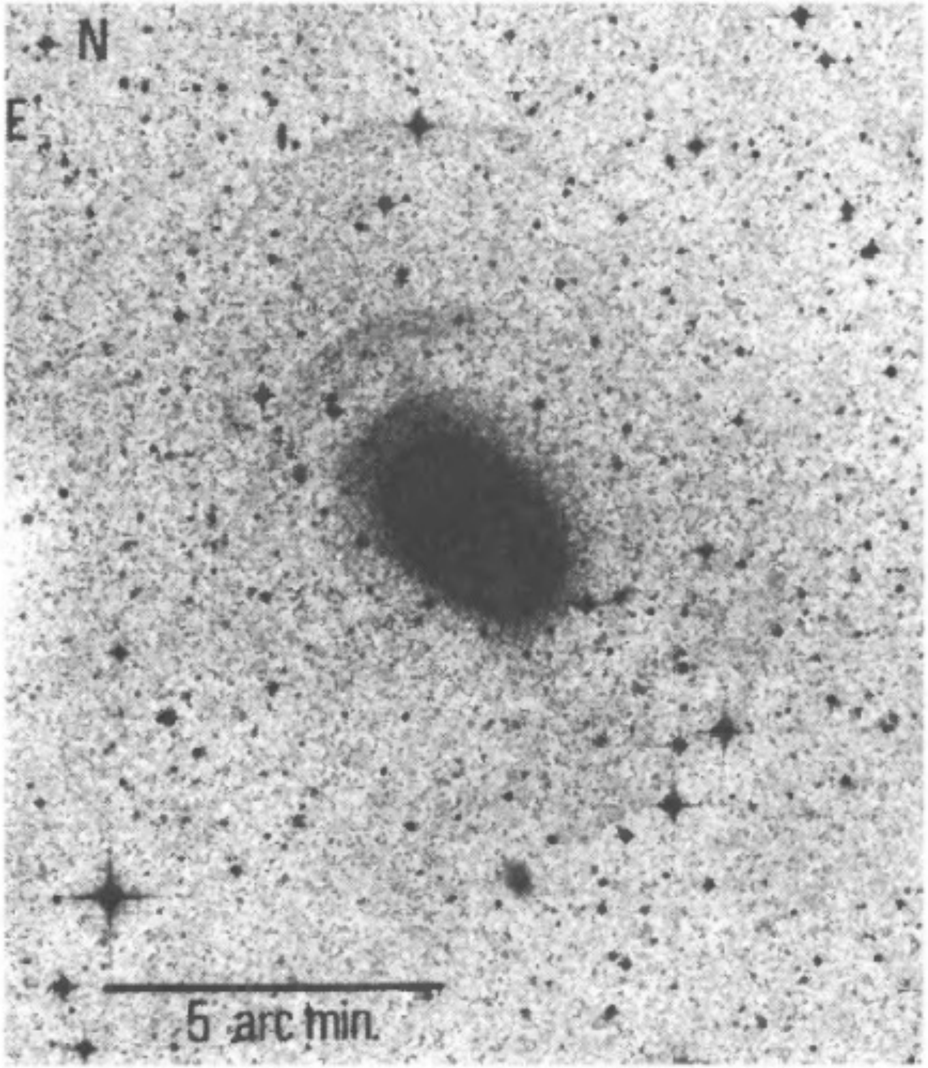

FIGURE 26.16 Faint concentric shells around the elliptical galaxy NGC 3923. (Figure from Malin and Carter, *Nature*, *285*, 643, 1980. Anglo-Australian Observatory photo by David Malin.)

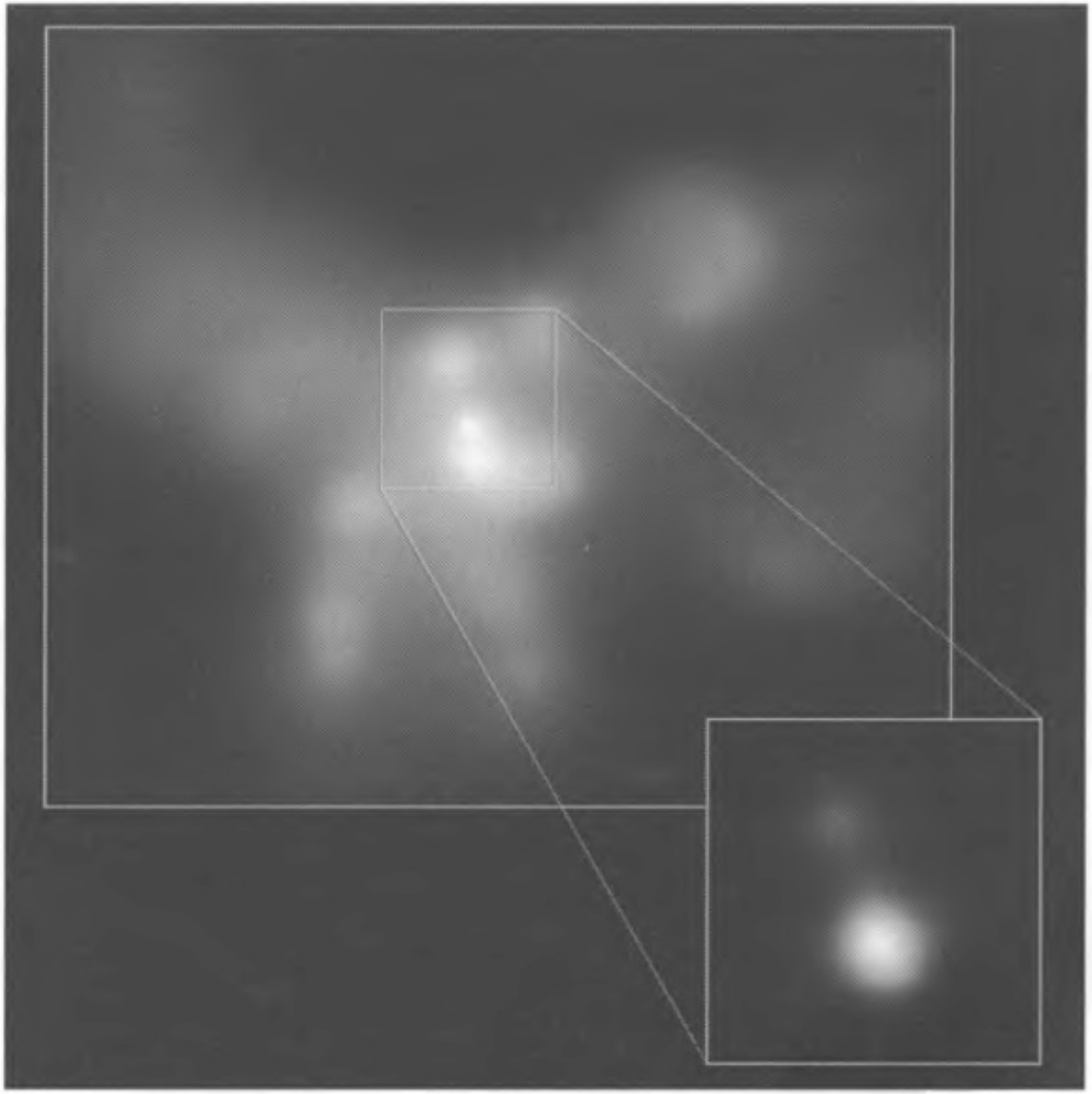

FIGURE 26.17 A Chandra X-Ray Observatory image of two supermassive black holes near the center of the "butterfly-shaped" galaxy, NGC 6240. (Courtesy of NASA/CXC/MPE/S. Komossa, et al.)

Formation of Galaxies: The Eggen, Lynden-Bell, Sandage Collapse Model

Their work was based on the following observations:

- Most metal poor stars have the highest eccentricities, the largest radial components of their peculiar motion (u), and the lowest angular momentum about the rotation axis of the Galaxy

- Metal rich stars tend to exist in near circular orbits on the plane.

The Basic Ingredients and predictions of the model:

- The Galaxy formed from the rapid collapse of a large proto-Galactic nebula.

- The old and low metallicity stars in the halo formed first while still on nearly radial trajectories, resulting in large u values.

- The halo stars are predicted to be metal poor since they formed first from material that has not been enriched by stellar nucleosynthesis.

- Collapse slowed when collisions between the gas and dust became more frequent.

- The nebula would rotate faster as it collapsed due the conservation of angular momentum and it would eventually form a disk of gas and dust and a young population of Pop I stars.

Formation of Galaxies: The Eggen, Lynden-Bell, Sandage Collapse Model

ELS model assumes:

- Free fall collapse of a cloud of uniform density ρ_0
- Spherical symmetry of collapse
- Isothermal gas: same temperature T during collapse. Typically T increases during collapse but if the density is low enough and the gas is optically thin photons can escape easily and radiate efficiently

From Newton's Second law and conservation of momentum

$$\rho \frac{d^2r}{dt^2} = -\frac{GM_r\rho}{r^2} - \frac{dP}{dr}$$

(left term is force over volume and the last term is zero for free fall)

M_r is the mass interior to the collapsing surface. This mass will remain constant during the collapse.

$$\frac{d^2r}{dt^2} = -G\left(\frac{\frac{4}{3}\pi r_0^3\rho_0}{r^2}\right)$$

Formation of Galaxies: The Eggen, Lynden-Bell, Sandage Collapse Model

$$\frac{d^2r}{dt^2} = -G\left(\frac{\frac{4}{3}\pi r_0^3 \rho_0}{r^2}\right) \Longrightarrow t_{ff} = \frac{\pi}{2\left[\frac{8\pi}{3}G\rho_0\right]^{\frac{1}{2}}}$$

Where t_{ff} is the free fall time for the cloud to collapse according to the ELS model.

Example: Assume a protogalactic cloud has a mass of $M = 5 \times 10^{11}\ M_\odot$ and $r_0 = 50$ kpc

The initial density is then $\rho_0 = \frac{M}{\frac{4}{3}\pi r_0^3} = 6.5 \times 10^{-23}$ kg/m^3

$$t_{ff} \sim 260 \text{ Myr}$$

Problems with ELS Model

1. **All halo stars and globular clusters** according to the ELS model **should be moving in the same direction** if they all formed from the collapse of a single nebula. **This is not what is observed**. About half of the outer-halo stars have retrograde orbits and their net rotation velocity is ~ 0 km/s The inner halo stars appear to have a net rotational velocity.

2. There is an **observed large range in the ages of globular clusters and halo stars of about 2 Gyears**. This is an order of magnitude longer than the collapse time of the ELS model.

3. **The ELS model predicts that globular clusters in the same galaxy should have similar metallicity**. This is not what is observed. Globular clusters near the galactic center are the more metal rich and the oldest. The globular clusters in the halo have a range of metallicities and are younger.

The Stellar Birthrate Function *B(M,t)*

$$B(M,t)dMdt = \psi(t)\xi(M)dMdt$$

B(M,t) is the stellar birthrate: Number of stars formed per unit volume with masses between *M* and *M* + *dM* and that are formed out of the ISM during the interval between *t* and *t*+*dt*

$\boldsymbol{\psi(t)}$ is the star formation rate (SFR): The mass of the ISM gas converted to stars per unit volume per unit time. For the disk of the Milky Way:

$$\psi(t) = 5 \pm 0.5\ \mathrm{M}_\odot\ \mathrm{pc}^{-2}\ \mathrm{Gyr}^{-1}$$

$\boldsymbol{\xi(M)}$ is the initial mass function (IMF): The number of stars with a mass between *M* and *M* + *dM*.

$$\xi(M) = \frac{dN}{dM} = cM^{-(1+x)}$$

for $7\ \mathrm{M}_\odot < M < 35\ \mathrm{M}_\odot$: $x \sim 1.8$
for $M > 40\ \mathrm{M}_\odot$: $x \sim 4$

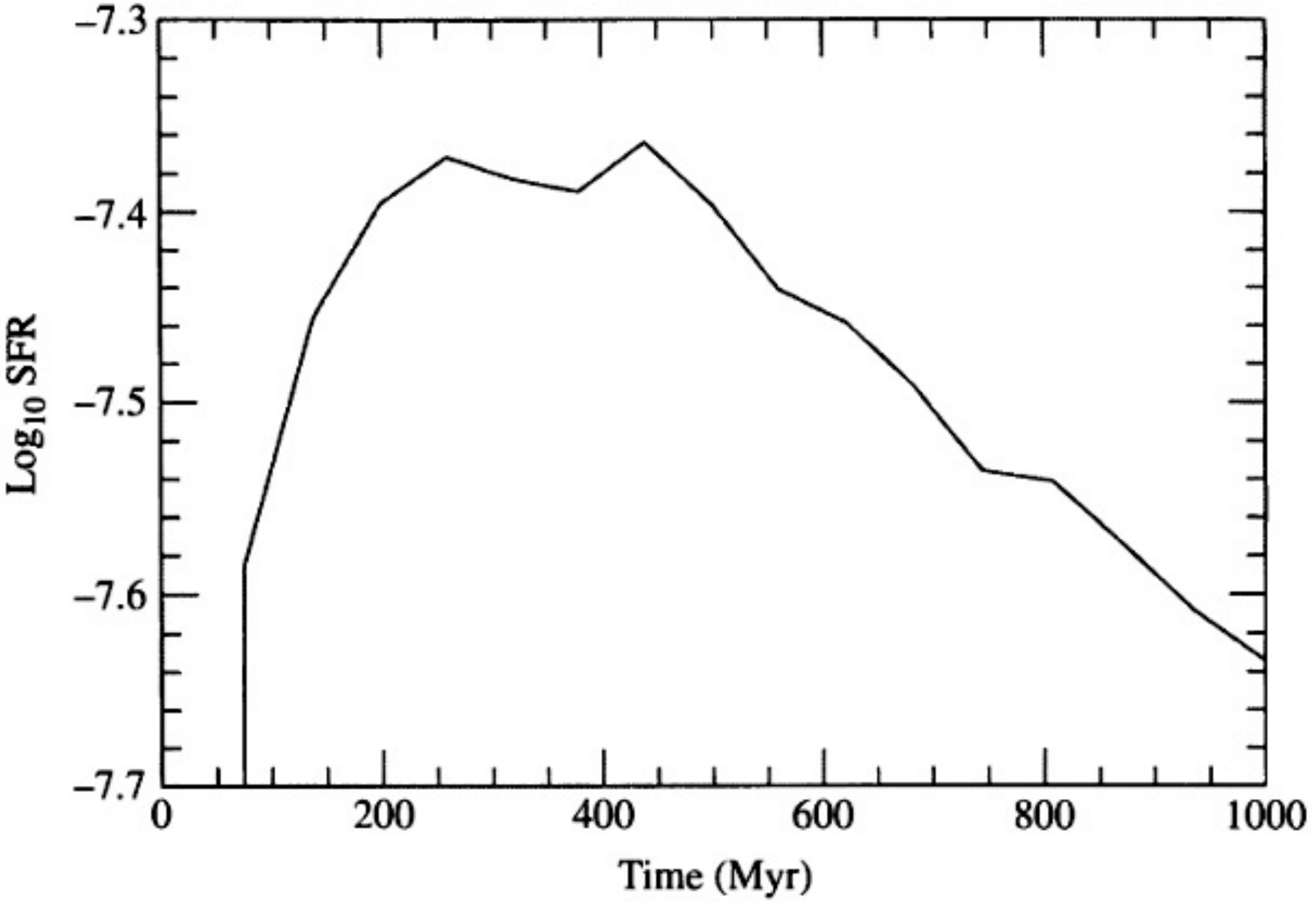

FIGURE 26.18 A model of the total star formation rate (in units of $M_\odot\ \mathrm{pc}^{-2}\ \mathrm{yr}^{-1}$) for the disk of the Milky Way Galaxy as a function of time. (Figure adapted from Burkert, Truran, and Hensler, *Ap. J.*, *391*, 651, 1992.)

A Dissipative Collapse Model

- A free fall collapse assumes $dP/dr = 0$ (that the gas can radiate energy efficiently). The time for collapse t_{ff} is referred to as the **dynamical timescale of collapse.**

- If the gas does not radiate efficiently then the timescale of collapse will depend on how long the gas takes to cool significantly.

If $t_{cool} >> t_{ff}$	gas cannot radiate energy fast enough for collapse to proceed. The gravitational energy gets converted to kinetic and thermal energy
If $t_{cool} << t_{ff}$	gas radiates efficiently and the nebular collapses in a free-fall timescale of t_{ff}

A Dissipative Collapse Model

The energy radiated per unit volume per unit time is:

$$r(t) = n^2 \Lambda(\mathrm{T})$$

$$\left(\frac{energy}{time \times volume}\right) = \left(\frac{1}{volume}\right)^2 \left(\frac{energy \times volume}{time}\right)$$

$\boldsymbol{\Lambda}(\mathbf{T})$ is called the **cooling function** and is the total energy radiated per unit time multiplied by the volume.

The time for all the energy to be radiated away from a protogalactic cloud of volume V is $\mathbf{t}_{\mathbf{cool}}$:

$$r(t)\boldsymbol{t}_{\boldsymbol{cool}}V = E_{total}$$

Estimate of t_{cool} for a Dissipative Collapse

The **total kinetic energy in the protogalactic cloud is:**

$$\text{KE}= \left(\frac{3}{2}kT_{virial}\right)N \quad (1)$$

where N is the total number of particles

$$\text{KE} = \left(\frac{1}{2}m_{ave}\langle v^2\rangle\right)N \quad (2)$$

$$(1) \wedge (2) \Rightarrow \left(\frac{3}{2}kT_{virial}\right) = \left(\frac{1}{2}m_{ave}\langle v^2\rangle\right) \Rightarrow T_{virial} = \frac{m_{ave}\sigma^2}{3k} = \frac{\mu m_H\sigma^2}{3k}$$

μ is called mean molecular weight and m_H is the mass of the hydrogen atom

$$r(t)\boldsymbol{t_{cool}}V = E_{total} = \left(\frac{3}{2}kT_{virial}\right)\text{N} \Rightarrow \boldsymbol{t_{cool}} = \frac{3}{2}\frac{kT_{virial}}{r(t)V} = \frac{3}{2}\frac{kT_{virial}}{n\Lambda(\text{T})}$$

Estimate of t_{cool} for a Dissipative Collapse

$\boldsymbol{t_{cool}} = \frac{3}{2}\frac{kT_{virial}}{n\Lambda(\mathrm{T})}$ and $T_{virial} = \frac{\mu m_H \sigma^2}{3k}$

The velocity dispersion of the atoms in a protogalactic gas can be calculated as follows:

$$-2\langle K\rangle = \langle U\rangle \Longrightarrow -2\frac{1}{2}m\langle v^2\rangle N = -\left(\frac{3GM^2}{5R}\right) \Longrightarrow N\mu m_H\sigma^2 = \left(\frac{3GM^2}{5R}\right) \Longrightarrow$$

$$\sigma^2 = \left(\frac{3GM}{5R}\right)$$

$\boldsymbol{t_{cool}} = \frac{3}{2}\frac{kT_{virial}}{n\Lambda(\mathrm{T})}$ and $T_{virial} = \frac{\mu m_H GM}{5kR}$

Example of Estimating t_{cool} of Dissipative Collapse

$$\boldsymbol{t_{cool}} = \frac{3}{2}\frac{kT_{virial}}{n\Lambda(\mathrm{T})} \quad \text{and } T_{virial} = \frac{\mu m_H GM}{5kR}$$

Assume a protogalactic cloud of $M = 5 \times 10^{11}\, M_\odot$, $R = 50$ kpc with 90% H and 10% He by number. First, we calculate the fraction by mass of H and He.

$$f_{mH} = \frac{90m_H}{90m_H+10m_{He}} = \frac{90m_H}{90m_H+40m_H} = \frac{90}{130} \sim 70\%$$

$$f_{mHe} = \frac{10m_{He}}{90m_H+10m_{He}} = \frac{40m_H}{90m_H+40m_H} = \frac{40}{130} \sim 30\%$$

$$\frac{1}{\mu} = 2\mathrm{X} + \frac{3}{4}\mathrm{Y} + \frac{1}{2}\mathrm{Z} \implies \mu = 0.6$$

$$T_{virial} = \frac{0.6\times(1.67\times10^{-27}\ \mathrm{kg})\times(6.67\times10-11\ \mathrm{m^3\,kg^{-1}\,s^{-2}})\times(5\times10^{11}\times2\times10^{30}\ \mathrm{kg})}{5\times(1.38\times10^{-23}\ \mathrm{J\,K^{-1}})\times(50\times3.09\times10^{19}\ \mathrm{m})} \implies$$

$T_{virial} = 6.2\times10^5$ K

Example of Estimating t_{cool} of Dissipative Collapse

$$\boldsymbol{t_{cool}} = \frac{3}{2}\frac{kT_{virial}}{n\Lambda(\mathrm{T})} \quad \text{and } T_{virial} = \frac{\mu m_H G M}{5kR}$$

$T_{virial} = 6.2\times10^{5}$ K

$n = \frac{\varrho}{\mu m_H} = \frac{3M}{4\pi R^3 \mu m_H} \sim 5\times10^{4}\ \mathrm{m}^{-3}$

$\Lambda(\mathrm{T}) \sim 1\times10^{-36}\ \mathrm{W\ m}^3$ for a temperature of $\mathrm{T} = 6.2\times10^{5}$ K

$$\boldsymbol{t_{cool}} = \frac{3}{2}\frac{(1.38\times10^{-23}\ \mathrm{J\ K}^{-1})(6.2\times10^{5}\ \mathrm{K})}{(5\times10^{4}\ \mathrm{m}^{-3})(1\times10^{-36}\ \mathrm{W\ m}^{3})} = 6.2\times10^{5}\,\mathrm{sec} \sim 8\ Myears$$

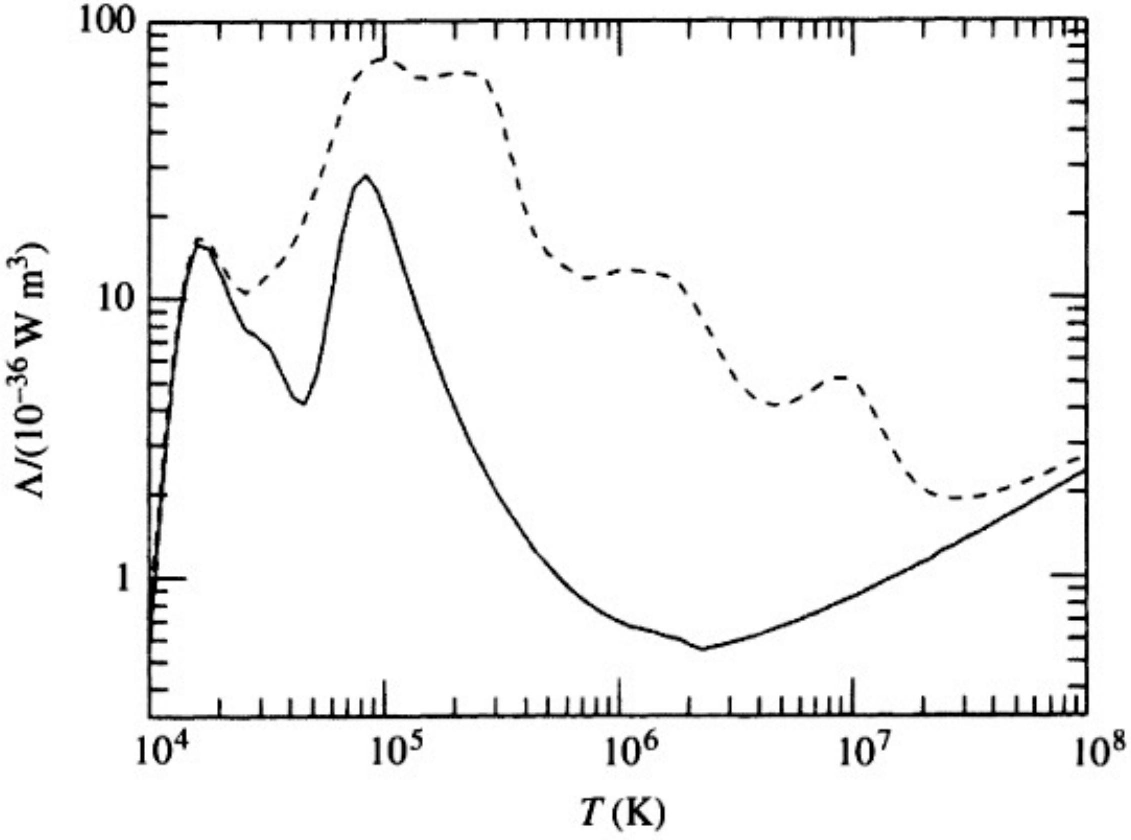

FIGURE 26.19 The cooling function $\Lambda(T)$. The solid line corresponds to a gas mixture of 90% hydrogen and 10% helium, by number. The dashed line is for solar abundances. (Figure adapted from Binney and Tremaine, *Galactic Dynamics*, Princeton University Press, Princeton, NJ, 1987.)

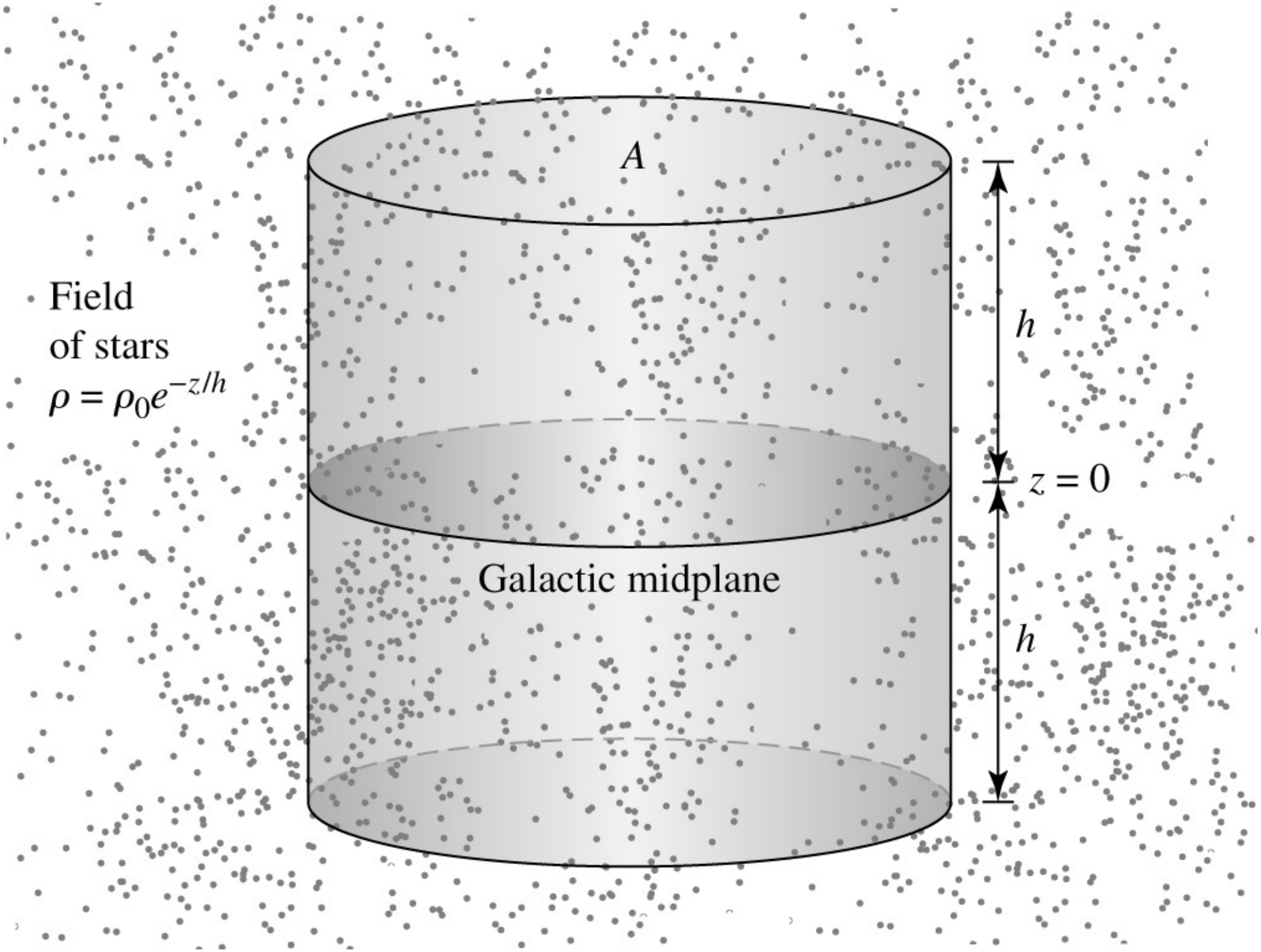
A
Field
of stars
$\rho = \rho_0 e^{-z/h}$
h
$z = 0$
Galactic midplane
h

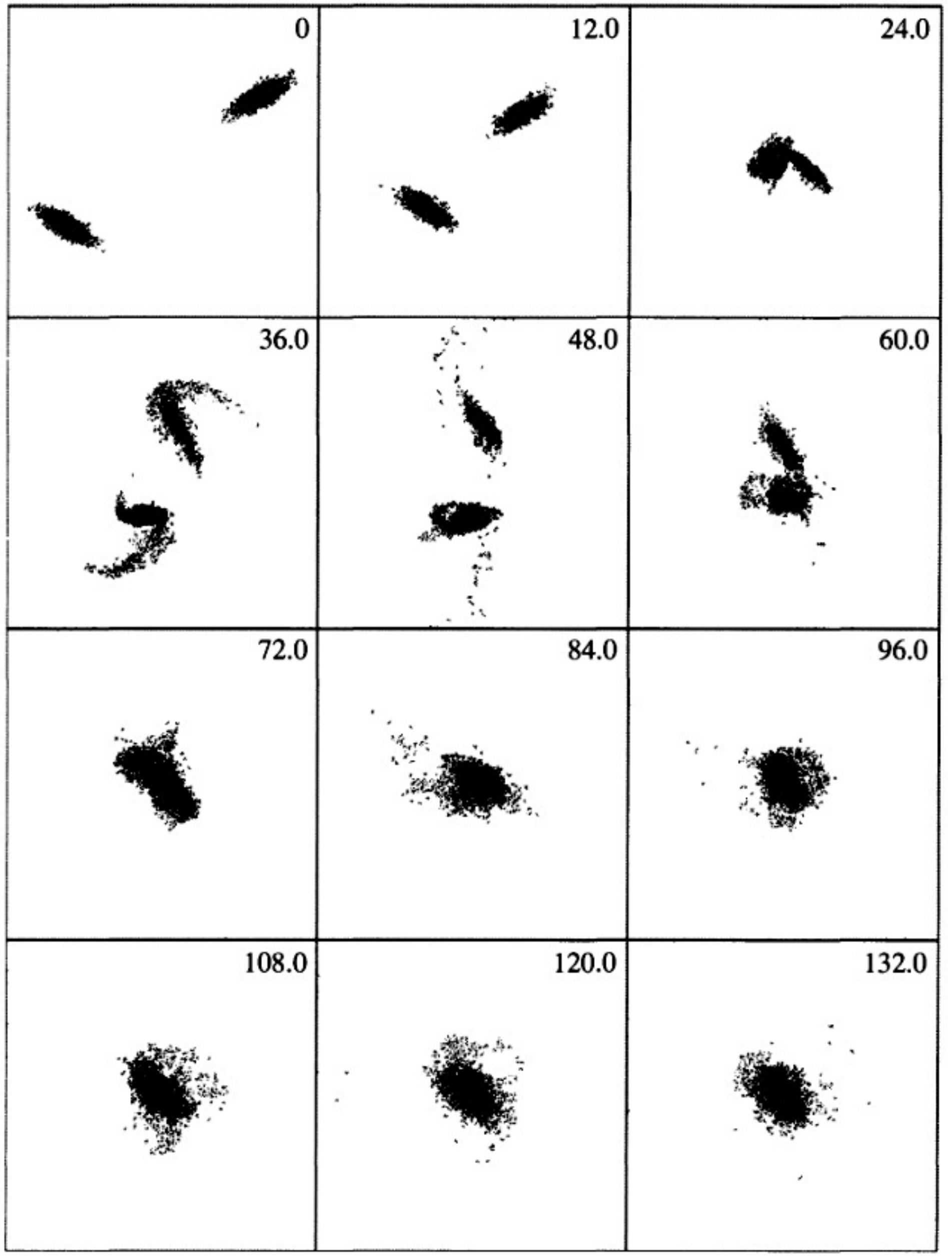

FIGURE 26.21 An N-body simulation of the merger of two spiral galaxies. Each disk is represented by 16,384 particles, and each bulge contains 4096 particles. The result is an elliptical galaxy with an $r^{1/4}$ profile. (Figure adapted from Hernquist, *Ap. J.*, *409*, 548, 1993.)

FIGURE 26.22 The Hubble Ultra Deep Field (HUDF), obtained by combining images from ACS and NICMOS onboard the HST. This HUDF image contains an estimated 10,000 galaxies covering a region 3 arcmin square (about 1/10 the size of the full moon) in the constellation Fornax. Some of the galaxies in the HUDF are so far away that we are seeing them less than 1 Gyr after the Big Bang. [Courtesy of NASA, ESA, S. Beckwith (STScI) and the HUDF Team.]

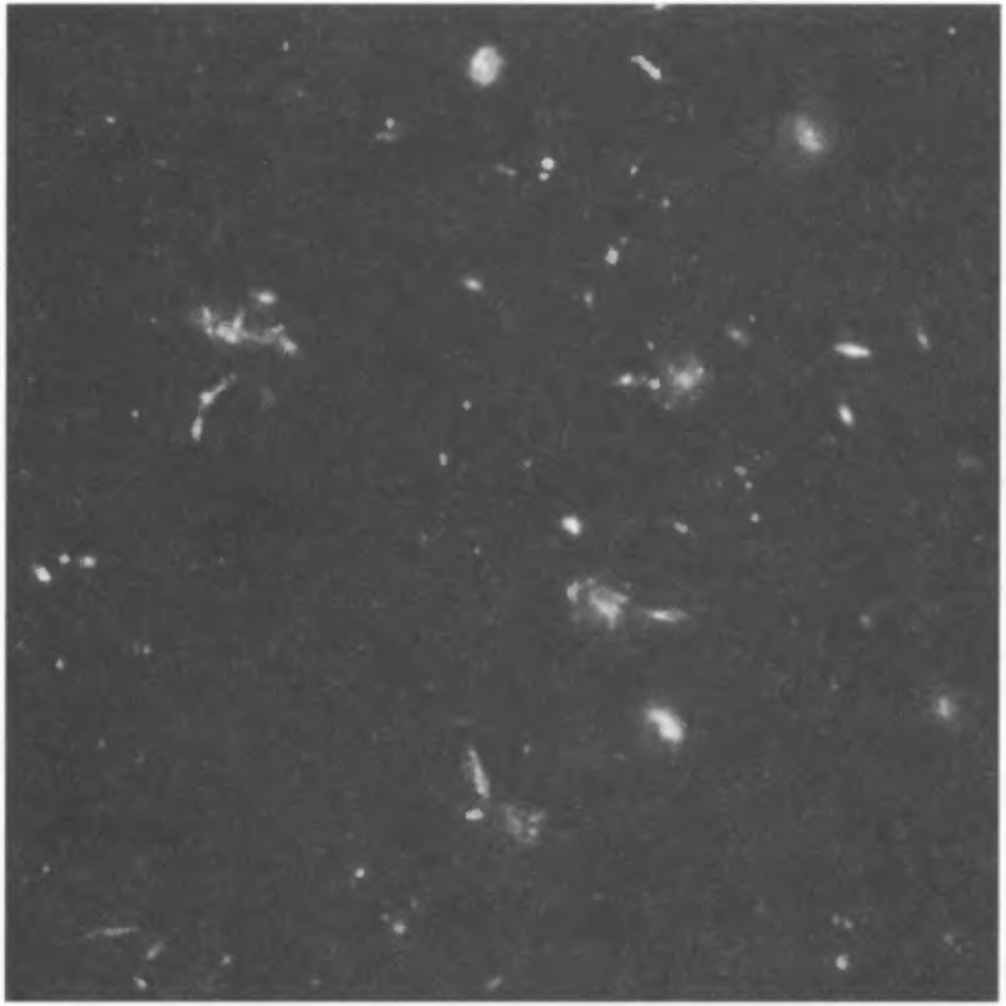

FIGURE 26.23 A close-up of a portion of the HUDF image shown in Fig. 26.22. Many of the galaxies in this image are extremely distant—and therefore extremely young. [Courtesy of NASA, ESA, S. Beckwith (STScI) and the HUDF Team.]

Detecting Dark Matter in Clusters of Galaxies

Example: The Bullet Cluster formed from the collision of two clusters

Using the weak lensing technique, astronomers have deduced that the dark mass in the clusters (blue) is separate from that of the hot gas.

This separation was presumably produced by the high-speed collision in which the **gas particles collided with each other, while the stars and dark matter were unaffected.**

This provides direct evidence that most of the matter in the Bullet Cluster is dark matter.

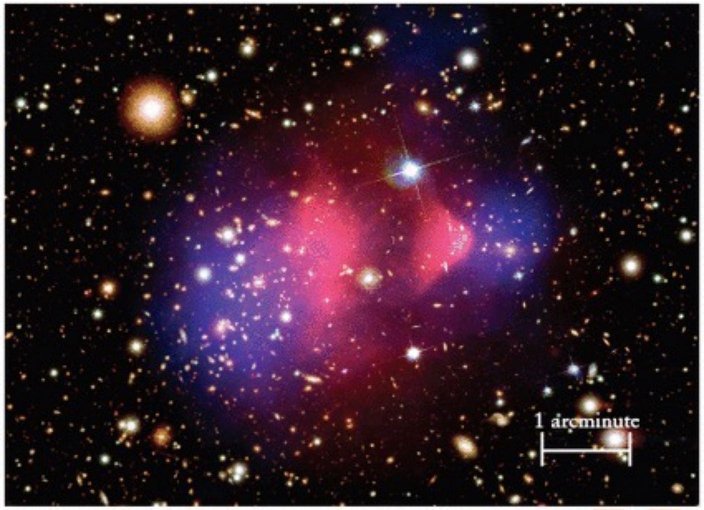

(a) Composite image of galaxy cluster 1E0657-56 showing visible galaxies, X-ray-emitting gas (red) and dark matter (blue)

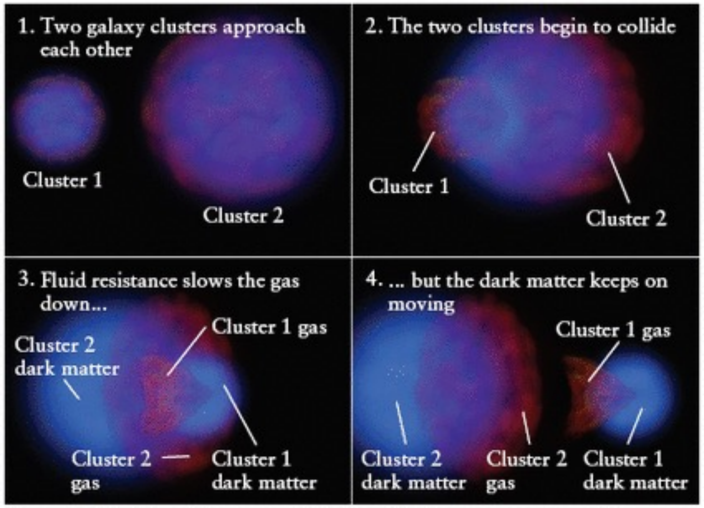

(b) A model of how the gas and dark matter in 1E0657-56 could have become separated

Formation of the First Galaxies

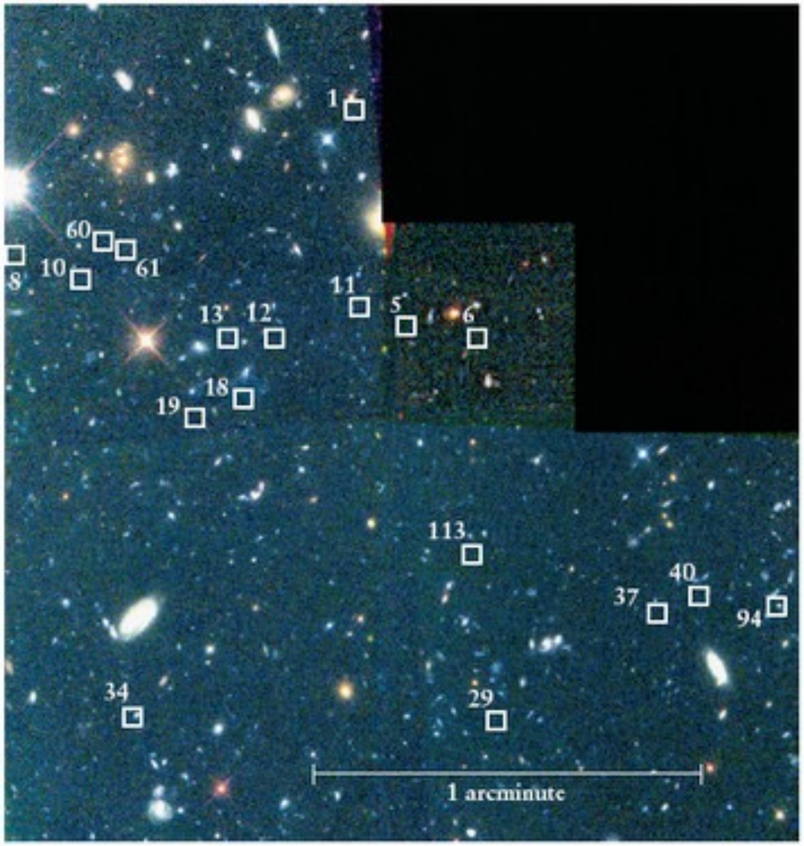

(a) A portion of the constellation Hercules

These very deep observations with HST show us how galaxies looked like in the distant past some ~11 billion years ago.

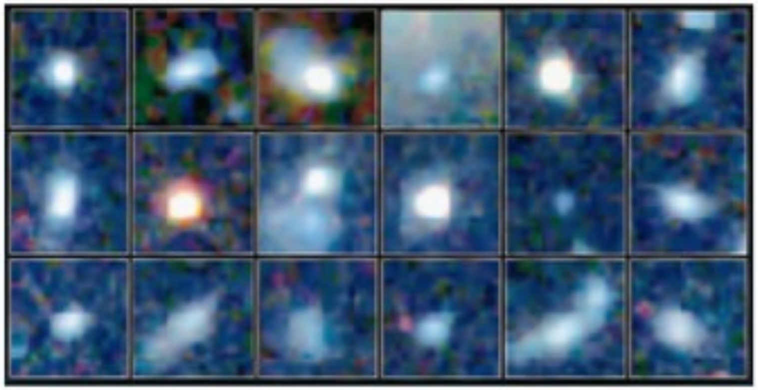

(b) Closeup images of the numbered objects in (a)

Recent observations of the very first galaxies in the Universe suggest that **galaxies formed from the merger of smaller objects**. This is often referred to as building galaxies from the "Bottom Up”. The building blocks of galaxies are about a few 1000 ly across.

The **very first galaxies appear very blue** indicating significant star formation at this time.

Spiral versus Elliptical Galaxies

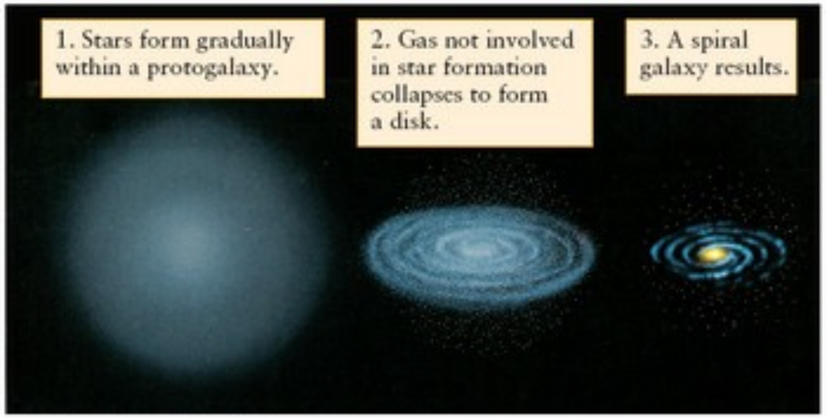

(a) Formation of a spiral galaxy

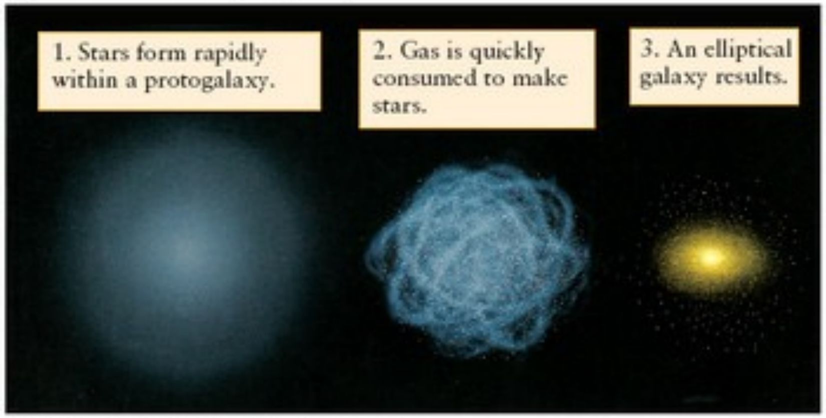

(b) Formation of an elliptical galaxy

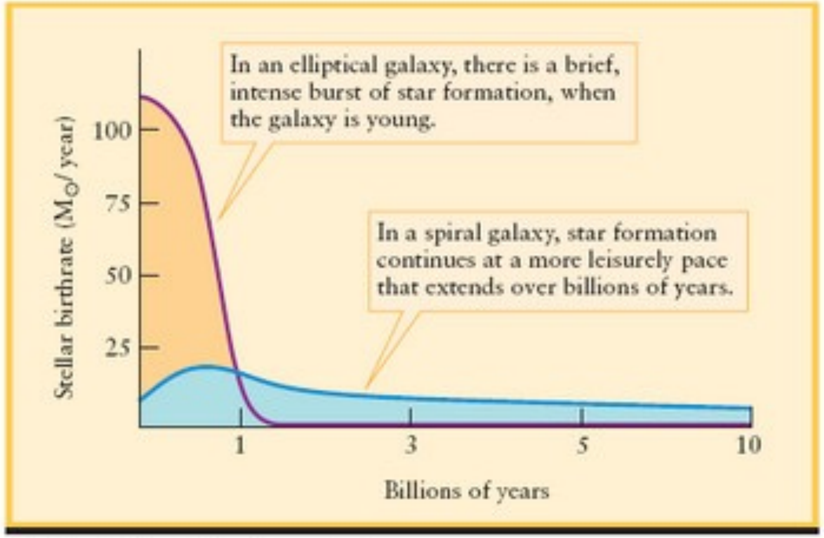

(c) The stellar birthrate in galaxies

One idea to explain why some galaxies become spirals and other ellipticals is that if star formation is large during the formation of the protogalaxy all the gas will be consumed quickly to form stars and no disk is formed resulting in an elliptical galaxy. Conversely, if star formation is weak within a protogalaxy the gas will have time to settle and form a disk resulting in a spiral galaxy.